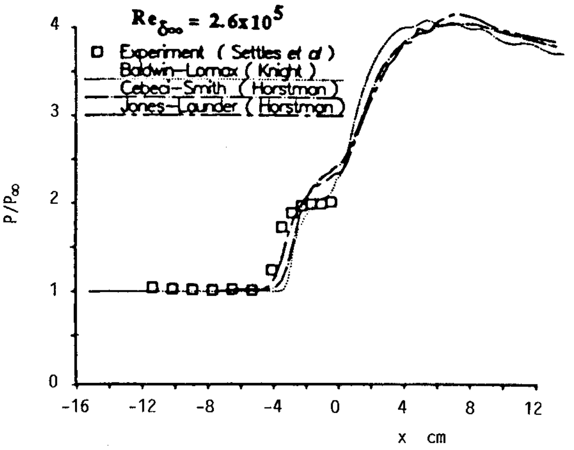


**Fig. 5 Supersonic turbulent flow at Mach 3 past a 40-deg swept 23-deg compression corner.**[5]

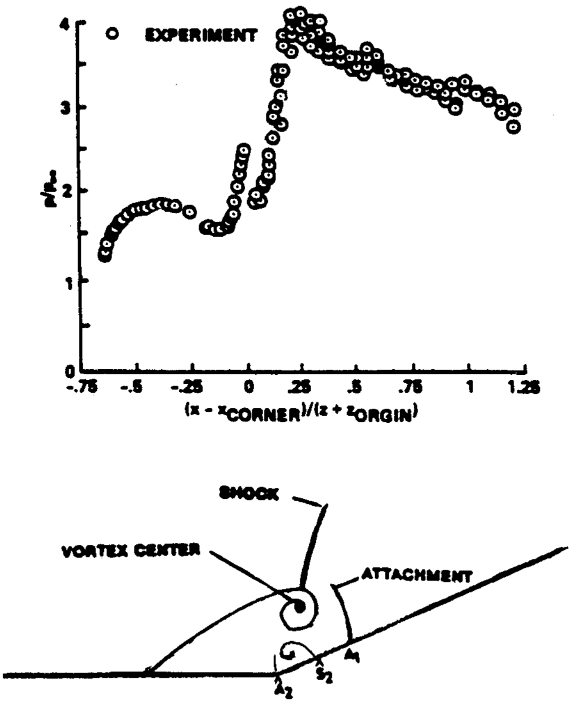


**Fig. 6 Suggested flowfield characteristics at Mach 3 for a 60-deg swept 23-deg compression corner.**

sent a realistic simulation of physical flow phenomena of concern. Fortunately, this danger is beginning to be recognized and demands are now being raised that with very few exceptions numerical simulation results should not be allowed to be published without the simultaneous presentation of results obtained by other means, e.g., by experiments. Only by diligent, intelligent use of physical and numerical experiments together can a realistic simulation of full-scale fluid mechanics be achieved.

## References


[1]Knight, D., Horstman, C. C., Ruderich, R., Mao, M.-F., and Bogdonoff, S., "Supersonic Turbulent Flow Past a 3-D Swept Compression Corner at Mach 3," AIAA Paper 87-0551, Jan. 1987.

[2]Fomison, N. R. and Stollery, J. L., "The Effects of Sweep and Bluntness of a Glancing Shock Wave Turbulent Boundary Layer Interaction," Paper 8, AGARD-CP-428, Nov. 1987.

[3]Ganzer, U. and Szodruch, J. "Vortex Formation Over Delta, Double-Delta and Wave Rider Configurations at Supersonic Speeds," Paper 25, AGARD-CP-428, Nov. 1987.

[4]Szodruch, J. and Monson, D. J., "Messung und Sichtbarmachung der leeseitigen Wandschubspannungen bei Deltaflügeln im Überschall," *Z. Flugwiss. Weltraumforsch,* Vol. 6, Heft 4. Vol. 6, 1982, pp. 279–283.

[5]Knight, D., Raufer, D., Horstman, C. C., and Bogdonoff, S., "Supersonic Turbulent Flow Past a Swept Compression Corner," AIAA Paper 88-0310, Jan. 1988.

[6]Pen, Y. S. and Probstein, R. F., "Rarefied Flow Transition at Leading Edge," *Fundamental Phenomena in Hypersonic Flow,* edited by J. G. Hall, Cornell University Press, Ithaca, NY, 1966, pp. 259–306.

[7]McCroskey, W. J., Bodgonoff, S. M., and McDougall, J. G., "An Experimental Model for the Leading Edge of a Sharp Flat Plate in Rarefied Hypersonic Flow," AIAA Paper 66-31, Jan. 1966.

[8]Shorenstein, M. L. and Probstein, R. F., "The Hypersonic Leading Edge Problem," AIAA Paper 68-4, Jan. 1968.

[9]Joss, W. W., Vas, I. E., and Bogdonoff, S. M., "Studies of the Leading-Edge Effect on the Rarefied Hypersonic Flow Over a Flat Plate," AIAA Paper 68-5, Jan. 1968.


# Free Rotation of a Circular Ring with an Unbalanced Mass


L. T. Watson*

*Virginia Polytechnic Institute and State University, Blacksburg, Virginia*

and

C. Y. Wang†

*Michigan State University, East Lansing, Michigan*


## Introduction

LARGE space structures are much more flexible than their terrestrial counterparts.[1] Rotation of large space structures may be desirable for stability, thermal, or artificial gravity reasons. Previous literature includes the large deformations due to the free rotation of a slender rod[2,3] and a ring about a diameter.[4]

An important model of a space station is a ring rotating about its axis of symmetry. If the ring is balanced, it will be stable and remain circular. The present Note considers the case when the ring is unbalanced by a mass attached to a point on the ring.

## Formulation

Figure 1 shows the origin of the coordinate system located on the symmetry line opposite a mass of magnitude $m$. The system is rotating in its own plane with angular velocity $\Omega$ about the center of mass. Normalize all lengths by the natural radius $R$ of the ring and all stresses by $EI/R^3$, where $EI$ is the flexural rigidity. The governing equation for large deformations is[5]

$$\theta'\theta'''' - \theta''\theta''' + \theta''(\theta')^3 - q_n\theta'' + q_t(\theta')^2 + q_n'\theta' = 0 \qquad (1)$$

where $\theta(s)$ is the local inclination, $s$ the arc length from the origin, and $q_n$ and $q_t$ the normal and tangential stresses caused by centrifugal forces. Consider an elemental length shown in Fig. 1. Let $\rho$ be the mass per unit length of the ring. We find $q_t = -Br\sin(\theta-\psi)$ and $q_n = Br\cos(\theta-\psi)$, where $r\cos\psi = h$

Received Feb. 1, 1988; revision received July 30, 1988. 


*Professor, Department of Computer Science.

†Professor, Departments of Mathematics and Mechanical Engineering.

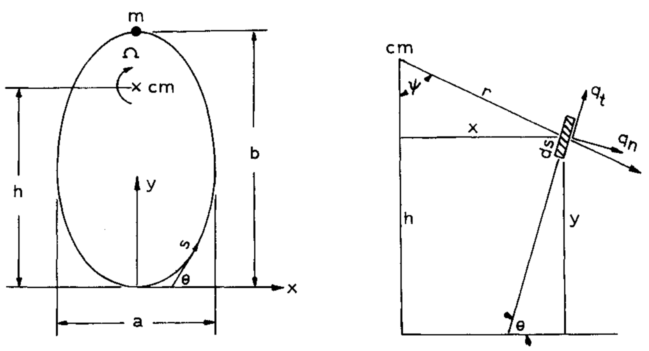


**Fig. 1 Coordinate system.**

$-y$, $r\sin\psi = x$, and $B = \rho\Omega^2 R^4/EI$ is the important nondimensional parameter representing the relative importance of rotation to flexibility. After some work, Eq. (1) becomes

$$\theta'\theta'''' - \theta''\theta''' + \theta''(\theta')^3 = B\{\theta''[(h-y)\cos\theta + x\sin\theta] + 2(\theta')^2[(h-y)\sin\theta - x\cos\theta]\} \tag{2}$$

Notice that $h$, the distance from the origin to the center of mass, is yet to be determined. The coordinates are related by

$$x' = \cos\theta, \qquad y' = \sin\theta \tag{3}$$

The bounday conditions for half the ring are

$$\theta(0) = x(0) = y(0) = \theta''(0) = 0 \tag{4}$$

$$x(\pi) = 0, \qquad \theta(\pi) = \pi \tag{5}$$

Balancing shear force at $s = \pi$ gives

$$\alpha \equiv \frac{m}{2\pi\rho R} = \frac{\theta''(\pi)}{\pi B[y(\pi) - h]} \tag{6}$$

where $\alpha$, the mass ratio, is the other important parameter. Given $B$ and $\alpha$, the sixth-order system [Eqs. (2) and (3)] with $h$ a variable is to be solved with the seven boundary conditions [Eqs. (4-6)].

## Perturbation for Small $B$

If $B$ is small, we can perturb from the circular state as follows:

$$\theta = s + B\phi(s) + \mathcal{O}(B^2) \tag{7}$$

$$x = \sin s + B\xi(s) + \mathcal{O}(B^2) \tag{8a}$$

$$y = 1 - \cos s + B\eta(s) + \mathcal{O}(B^2) \tag{8b}$$

The leading orders of Eqs. (2–5) are

$$\phi'''' + \phi'' = 2(h-1)\sin s \tag{9a}$$

$$\xi' = -\phi\sin s \qquad \eta' = \phi\cos s \tag{9b}$$

$$\phi(0) = \xi(0) = \eta(0) = \phi''(0) = \xi(\pi) = \phi(\pi) = 0 \tag{10}$$

$$\alpha = \frac{\phi''(\pi)}{\pi(2-h)} \tag{11}$$

The solution is

$$\phi = \frac{\alpha}{\alpha+1}\left(s\cos s + s - \frac{3}{2}\sin s\right) \tag{12}$$

$$\xi = \frac{\alpha}{\alpha+1}\left(\frac{1}{4}s\cos 2s - \frac{1}{8}\sin 2s + s\cos s - \sin s + \frac{3}{4}s - \frac{3}{8}\sin 2s\right) \tag{13}$$

$$\eta = \frac{\alpha}{\alpha+1}\left(\frac{1}{4}s\sin 2s + \frac{1}{2}\cos 2s + s\sin s + \cos s + \frac{s^2}{4} - \frac{3}{2}\right) \tag{14}$$

$$h = \frac{2\alpha+1}{\alpha+1}. \tag{15}$$

Thus, the normalized moments are

$$\theta'(0) = 1 + \frac{\alpha}{2(\alpha+1)}B + \mathcal{O}(B^2) \tag{16a}$$

$$\theta'(\pi) = 1 + \frac{3\alpha}{2(\alpha+1)}B + \mathcal{O}(B^2) \tag{16b}$$

The maximum length $b$ is

$$b = y(\pi) = 2 + \frac{\alpha}{\alpha+1}\left(\frac{\pi^2}{4} - 2\right)B + \mathcal{O}(B^2) \tag{17}$$

For the maximum width $a$, first find the location $s = s^*$ such that $\theta(s^*) = \pi/2$. From Eqs. (7) and (12),

$$s^* = \frac{\pi}{2} - \frac{\alpha}{2(\alpha+1)}(\pi - 3)B + \mathcal{O}(B^2) \tag{18}$$

Then,

$$a = 2x(s^*) = 2 - \frac{2\alpha}{\alpha+1}\left(1 - \frac{\pi}{4}\right)B + \mathcal{O}(B^2) \tag{19}$$

## Numerical Integration

For general $B$, Eqs. (2-5) are converted to a nonlinear system of equations as follows: let $v = [\theta'(0), \theta'''(0)]^t$ and let $x(\eta;v)$, $y(\eta;v)$, and $\theta(\eta;v)$ denote the solution to the initial value problem with initial conditions [Eq. (4)] and $v$, assuming $h$ is fixed. Then, the two-point boundary value problem (for fixed $h$) is equivalent to the problem of finding the initial conditions $v$ such that $F(v) = [x(\pi;v), \theta(\pi;v) - \pi]^t = 0$. Note that $F(v)$ is an implicit highly nonlinear function of $v$. The system of equations is solved by a globally convergent homotopy method, which has been described theoretically[6] and algorithmically.[7] The mathematical software package HOMPACK[7] was used to perform the computation. This homotopy approach in conjunction with nonstandard shooting has been described elsewhere[8] and so will not be repeated here.

Solving the nonlinear system requires partial derivatives such as $\partial x(\pi;v)/\partial v_1$ (or approximations thereof). These partial derivatives can be accurately and efficiently computed as follows. Let

$$Y = \left(x, y, \theta, \theta', \theta'', \theta''', \frac{\partial x}{\partial v_i}, \frac{\partial y}{\partial v_i}, \frac{\partial \theta}{\partial v_i}, \frac{\partial \theta'}{\partial v_i}, \frac{\partial \theta''}{\partial v_i}, \frac{\partial \theta'''}{\partial v_i}\right)$$

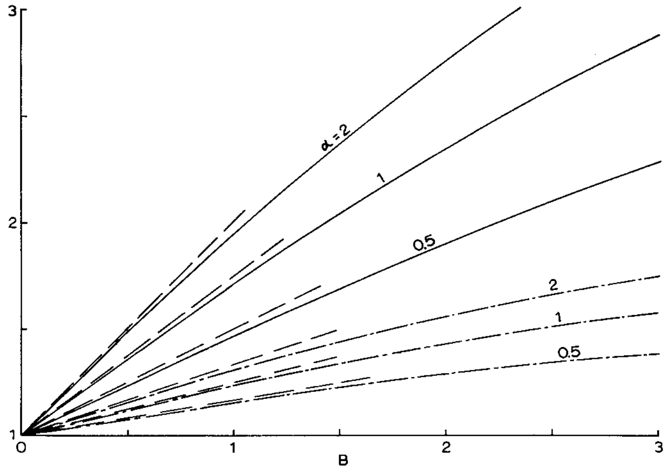


Fig. 2 Curvature or normalized moment as a function of $B$ for various $\alpha$:——, $\theta'(\pi)$; — · — · —, $\theta'(0)$; — — — —, approximations Eqs. (16).

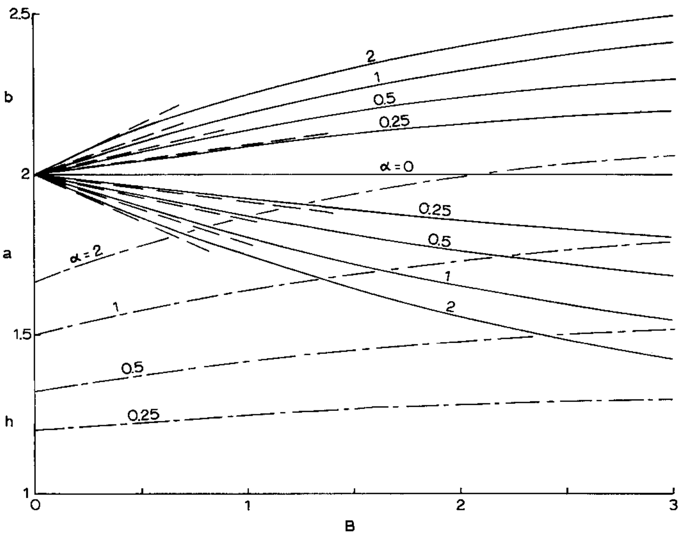


Fig. 3 Maximum length $b$ and maximum width $a$: — · — · —, distance $h$ to center of mass; — — — —, approximations Eq. (17) or Eq. (19).

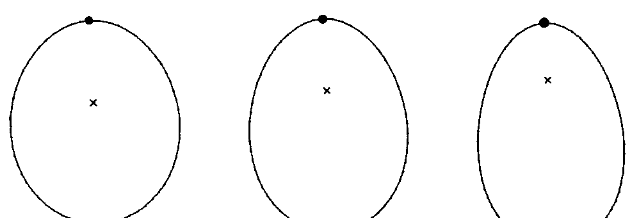

Fig. 4 Configurations for the same rotation rate $B=2$ (from left to right $\alpha=0.25$, 0.5, and 1, cross indicates center of mass).

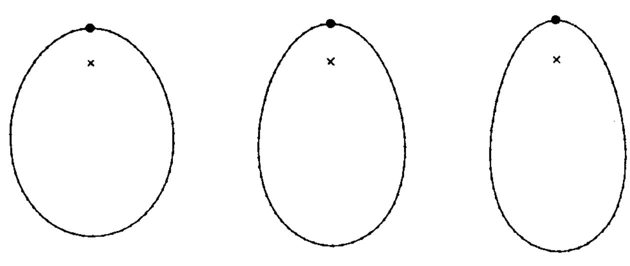

Fig. 5 Configurations for the same mass $\alpha=2$ (from left to right $B=1$, 2, and 3, cross indicates center of mass).

which is the solution of the first-order initial value problem

$$Y_1' = \cos Y_3, \quad Y_5' = Y_6, \quad Y_9' = Y_{10}$$

$$Y_2' = \sin Y_3, \quad Y_6' = T/Y_4, \quad Y_{10}' = Y_{11}$$

$$Y_3' = Y_4, \quad Y_7' = (-\sin Y_3)Y_9, \quad Y_{11}' = Y_{12}$$

$$Y_4' = Y_5, \quad Y_8' = (\cos Y_3)Y_9,$$

$$Y_{12}' = (Y_4 T' - T Y_{10})/Y_4^2$$

$$Y(0) = (0,0,0,v_1,0,v_2,0,0,0,\delta_{1,i},0,\delta_{2,i})$$

where

$$T = Y_5 Y_6 - Y_5 Y_4^3 + B\{ Y_5[(h-Y_2)\cos Y_3 + Y_1 \sin Y_3] + 2Y_4^2[(h-Y_2)\sin Y_3 - Y_1 \cos Y_3]\}$$

and $T' = \partial T/\partial v_i$. For example, integrating this system with $i=1$ up to $\eta=\pi$ gives $Y_7(\pi) = \partial x(\pi;v)/\partial v_1$.

However, the constant $h$ must satisfy $h = y(\pi,v) - \theta''(\pi;v)/(\pi B\alpha)$, which is simply a nonlinear scalar equation for $h$. So, the overall algorithm is 1) fix a value for $h$; 2) solve $F(v) = 0$ for $v$ (keeping $h$ fixed); 3) compute $y(\pi;v)$ and $\theta''(\pi;v)$; 4) if the equation for $h$ is satisfied, stop. Otherwise, adjust the value of $h$ using the secant method and return to step 2.

It would have been possible to formulate the entire problem as a single nonlinear system in the three unknowns $v_1$, $v_2$, and $h$ and simultaneously solve for $v$ and $h$. The above decoupling is more efficient computationally, however.

## Discussion of Results

Figure 2 shows the curvatures or normalized moments. The maximum moment occurs at $s=\pi$ or at the location of the point mass. Of much smaller magnitude is the moment at $s=0$. Both moments increase with $\alpha$ and $B$. Our approximate formulas compare well with exact numerical integration for $B<1$. Figure 3 shows the maximum length $b$ increases with $\alpha$ and $B$ while the maximum with $a$ decreases. Both Figs. 2 and 3 are useful in the design of freely rotating rings. Figures 4 and 5 show the deformed configurations of the ring for some values of $\alpha$ and $B$. We see the shape is neither circular nor elliptic but egg shaped.

## References

[1]Ashley, H., "Observations on the Dynamic Behavior of Large Flexible Bodies in Orbit," *AIAA Journal*, Vol. 5, March 1967, pp. 460–469.

[2]Wang, C. Y., "Rotation of a Free Elastic Rod," *Journal of Applied Mechanics*, Vol. 49, March 1982, pp. 225–227.

[3]Wang, C. Y., "Equilibrium Configurations and Energies of the Rotating Elastic Cable in Space," *AIAA Journal*, Vol. 24, Dec. 1986, pp. 2010–2013.

[4]Wang, C. Y. and Watson, L. T., "Free Rotation of a Circular Ring About a Diameter," *Journal of Applied Mathematics and Physics*, Vol. 34, Jan. 1983, pp. 13–24.

[5]Wang, C. Y., Watson, L. T., and Kamat, M. P., "Buckling, Postbuckling and the Flow Through a Tethered Elastic Cylinder under External Pressure," *Journal of Applied Mechanics*, Vol. 50, March 1983, pp. 13–18.

[6]Watson, L. T., "Numerical Linear Algebra Aspects of Globally Convergent Homotopy Methods," *SIAM Review*, Vol. 28, Dec. 1986, pp. 529–545.

[7]Watson, L. T., Billups, S. C., and Morgan, A. P., "Algorithm 652: HOMPACK: A Suite of Codes for Globally Convergent Homotopy Algorithms," *ACM Transactions on Mathematical Software*, Vol. 13, Sept. 1987, pp. 281–310.

[8]Heruska, M. W., Watson, L. T., and Sankara, K. K., "Micropolar Flow Past a Porous Stretching Sheet," *Computers and Fluids*, Vol. 14, No. 2, 1986, pp. 117–129.